

**Characteristic intra- and interunit interactions of Kr atoms adsorbed on the Si(111)-7×7 surface**Yan Jun Li, Osamu Takeuchi, Don N. Futaba, Haruhiro Oigawa, Koji Miyake,\* and Hidemi Shigekawa†  
*Institute of Applied Physics, 21st Century COE, University of Tsukuba, Tsukuba 305-8573, Japan*

Young Kuk

*Department of Physics and Center for Science in Nanometer Scale, Seoul National University, Seoul 151-742, Korea*

(Received 9 September 2002; revised manuscript received 23 December 2002; published 3 July 2003)

Adsorption of Kr atoms on the Si(111)-7×7 surface at 8 K was studied by scanning tunneling microscopy. Despite similar electronic structures of noble gas atoms, the observed site-dependent adsorbed Kr structures and their formation processes were different from those of Xe atoms. In comparison with the results of simulation, the existence of the characteristic intraunit and interunit interactions between Kr atoms was confirmed.

DOI: 10.1103/PhysRevB.68.033301

PACS number(s): 68.43.Fg, 68.37.Ef

In recent molecular devices, molecular layers are deposited on metal or semiconductor substrates. When they are deposited on surfaces, we do expect a strong interaction between the molecular layers and substrates. Therefore, the understanding and control of the interaction between molecules and substrate surfaces has become an important issue. Noble gas atoms on various substrates have been model systems for studying the interaction because of their simple electronic structure.

Recent scanning tunneling microscopy (STM) studies have revealed characteristic interaction mechanisms of rare gases on metal and semiconductor surfaces.<sup>1–6</sup> For example, Xe atoms on Pt(111) and Cu(111) surfaces show completely different adsorption behaviors despite the similarity of the substrate geometries. The complicated interactions between rare gases can be interpreted as follows. The adsorption of rare gases influences the substrate electronic structures, which then leads to a change in the electronic structure of the adsorbates, resulting in the observed adsorption processes. In fact, recently, the dispersion of the Cu surface state was found to be modified by Xe adsorption.<sup>5</sup> In addition, Xe atoms were found to form site-dependent adsorption structures on the Si(111)-7×7 surface. The  $I/V$  characteristic of STM images and the stability of Xe atoms under STM scanning also showed a considerable site dependence, which is a direct indication of the occurrence of interactions between Xe and Si substrate atoms.<sup>6</sup> The observed characteristic properties are difficult to explain, in consideration of the stable electronic structures of the rare gases and of the fact that they have been adopted as a model for analyzing the interaction of ideal gases even on metal surfaces.

In order to clarify the point described above, we analyzed the adsorption processes of another rare gas, Kr, on the Si(111)-7×7 surface by STM at 8 K. Despite similar electronic structures of noble gas atoms, the observed site-dependent adsorbed Kr structures and their formation processes were different from those of Xe atoms. In comparison with the theoretical calculation, the existence of the characteristic intraunit and interunit interactions between Kr atoms on Si(111)-7×7 surface was confirmed for the first time.

The samples used were As-doped,  $n$ -type Si(111) surfaces with a conductivity of 0.37–0.625  $\Omega$  cm. The base pressure

was  $7 \times 10^{-9}$  Pa. After confirming a complete 7×7 structure, the sample was cooled to 8 K. The STM tip was retracted from the sample during gas exposure, and observation was carried out over the same area after adsorbing Kr. An electrochemically etched tungsten tip was used. We observed various areas of the samples with different doses in order to check the reproducibility. The coverage was determined from the observed STM images. The dosing rate of Kr gas was controlled with an electronically controlled pulse valve. The sample temperature was monitored using an Au + 0.07% Fe-Cr thermocouple located near the sample.

Figure 1(a) shows a typical STM image of the Kr adsorbed surface. Although adsorbed Kr atoms still diffused during STM observation, the stability was sufficient to observe the structures at this low coverage. Kr atoms are dominantly adsorbed in the faulted-half (FH) units. In the unfaulted-half (UH) units, three different structures were observed, the magnified images of which are shown in Figs. 1(b)–1(d). As represented by the schematic models in Fig. 1, these structures consist of the one dimer+one corner Kr atom ( $1D+1C$ ) structural unit which is the same structure as that observed in the case of Xe.<sup>6</sup> However, despite the same final structure,  $3D+3C$ , the adsorption processes were different for Kr. Xe atoms first adsorb in a dimer form, resulting in the hexagonal shape formed by three dimers (six green circles in Fig. 1). The three corner sites (three yellow circles in Fig. 1) are then occupied one by one. However, the adsorption of Kr proceeds in units of Kr trimers, that is, the  $1D+1C$  structure in the notation used for Xe: (1) one trimer, (2) two trimers and (3) three trimers. In detail, a one-trimer structure can also sometimes be found in the Xe case when the neighboring half-unit is occupied by Xe atoms. In addition, the  $3D+2C$  structure can also be found in the Kr case. However, the major growth modes are clearly different; that in the Xe case is based on dimer adsorption and that in the Kr case is based on trimer adsorption.

In the FH units, the observed structures were even more different from those of Xe. In the case of Xe, the same structure,  $3D+3C$ , was also formed in the FH units. However, as shown in Fig. 2, four types of different adsorption structures were dominantly observed for Kr: (a) a base structure ( $B$ ) and (b) one ( $1Ce$ ), (c) two ( $2Ce$ ), and (d) three adatoms

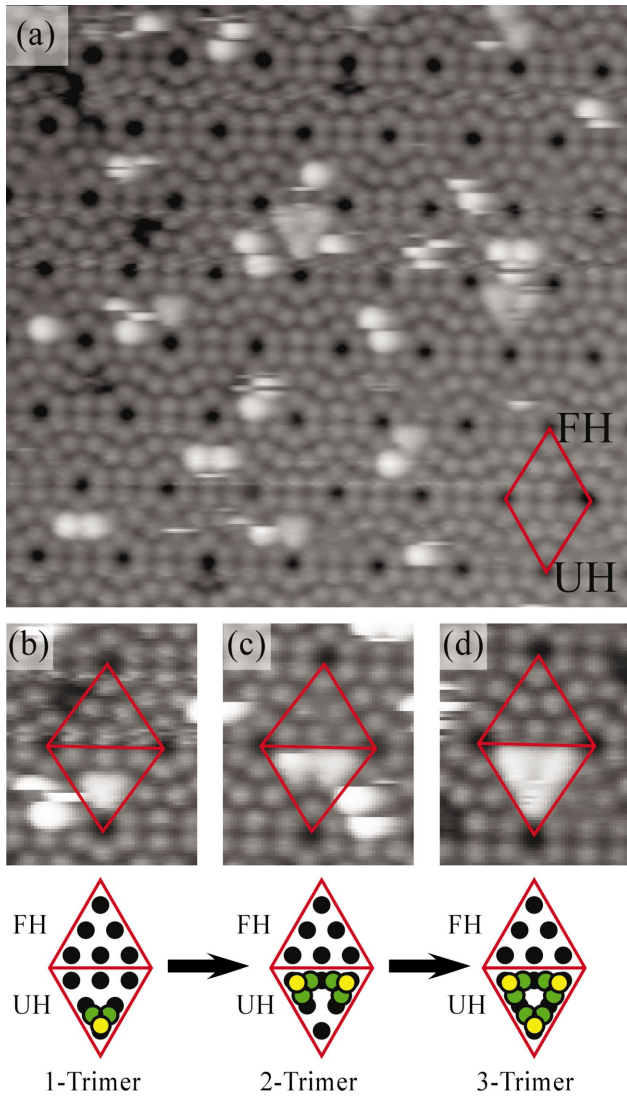


FIG. 1. (Color) (a) A typical STM image of Kr adsorbed Si(111)- $7\times 7$  surface at 8 K ( $V_s=2$  V,  $I_t=0.3$  nA). (b) 1-trimer, (c) 2-trimer, and (d) 3-trimer structures.

(3Ce) at the center adatom site. The base structure is rather unclear at this bias voltage. Compared to the clean FH units [yellow triangle in Fig. 2(a)], however, the image of this structure is slightly brighter in the area between Si adatoms. The difference is much clearer when the bias voltage is changed from 2.0 to 3.0 V [Fig. 3(a)]. In this figure the Kr adatoms at the center adatom site diffuse across the surface, which appears in the image as horizontal bright streaks indicated by a white arrow. However, it is obvious that they are always on the base structure. Thus, we concluded that when Kr adatoms are observed at the center adatom site, the base structure always exists below them, which is the reason for the notation. Therefore, they are written as (b)  $B+1Ce$ , (c)  $B+2Ce$ , and (d)  $B+3Ce$  in Fig. 2. The details of the base structure are discussed later. In addition to these structures, further Kr adsorption was sometimes observed on the corner adatom sites, as shown in Fig. 2(e). Consequently, the final structure of adsorbed Kr atoms in the FH structure is expected to be six Kr atoms adsorbed on center and corner sites

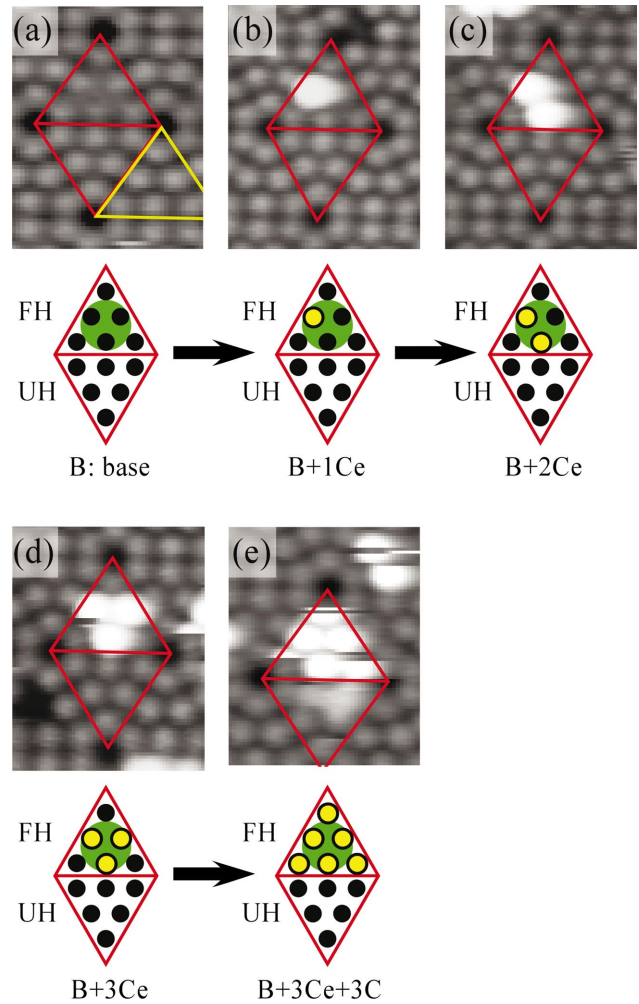


FIG. 2. (Color) STM images of Kr adsorbed Si(111)- $7\times 7$  FH unit at 8 K: (a) base structure and structures with (b) single (c) two, and (d) three Kr atoms at the center adatom sites. (e) FH unit with six Kr atoms at the center and corner adatom sites.

with the base structure existing below them [Fig. 2(e):  $B+3Ce+3C$ ].

To illustrate the difference between Xe and Kr in their adsorption processes, a simple rigid ball model was built similarly as in the case of Xe adsorption.<sup>6</sup> When Kr atoms that form dimers were located at the same positions as Xe atoms, i.e., in contact with a rest atom, its neighboring center adatom, and one of the Si atoms to which the center adatom is bonded, the calculated distance between the two Kr atoms is approximately 0.44 nm, which is significantly larger than the diameter of the Kr atom, 0.41 nm. This disagreement might have caused the instability of the isolated dimer adsorbate, contrary to the Xe case, which results in the growth mode based on trimer units in UH units and a completely different structure in FH units. Indeed, the completely different growth mode in the UH unit is quite noteworthy. Since the calculated positions are almost the same for the two units, the observed phenomenon indicates that Kr more sensitively reflects the difference in the electronic structures of FH and UH units.

Figure 3 shows magnified images of the base structure at

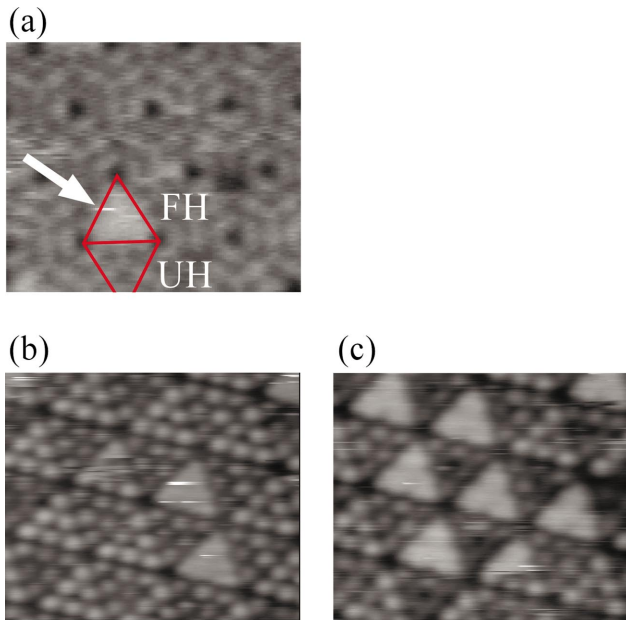


FIG. 3. (Color) FH unit with the base structure observed at sample bias voltages of (a) 3 V, (b)  $-1.5$  V, and (c)  $-2$  V.

different sample bias voltages (3,  $-1.5$ , and  $-2$  V). First, at higher voltages, the trimer Kr atoms in UH units and the upper center and corner Kr atoms in FH units became unstable under STM scanning, indicating their weaker interaction with the substrate compared to Kr atoms in the base structure in the FH units. With the sample bias of 2 V, as mentioned above, the base structure is imaged with a fuzzy outline [Fig. 2(a)]. At 3 V, the contrast becomes clearer, but a detailed structure does not appear, as shown in Fig. 3(a). On the other hand at negative sample bias voltages, the base structure is imaged clearly even at  $-1.5$  V [Fig. 3(b)]. In particular, at  $-2$  V, the base structure is imaged separately into three parts near corner adatom sites, as shown in Fig. 3(c). Moreover, only one or two of the three parts are sometimes observed in a FH unit cell [an example is shown in Fig. 3(c)]. Although the details cannot be determined, a possible origin of the base structure is three dimer Kr atoms (three green atoms in the schematic model in Fig. 2) and additional Kr atoms in the hexagonal Kr dimer structure. In any case, the adsorption of the structure modifies the center adatom sites to be more attractive to the subsequent Kr atoms.

In order to understand intra- and inter-half-unit interactions of Kr gases in detail, we analyzed the distribution of Kr atoms. First, the interaction in a half-unit, intra- $7 \times 7$ -half-unit interaction, is investigated. Figure 4(a) shows the distribution of the number of Kr atoms at center adatom sites in a FH unit with base structure (red line). Schematic adsorption structures of type-0 ( $B$ ), type-1 ( $B+1Ce$ ), type-2 ( $B+2Ce$ ), and type-3 ( $B+3Ce$ ) are also shown below the graphs. When the distribution of Kr atoms is completely random, the distribution will be  $N(1-\theta)^3$ ,  $3N\theta(1-\theta)^2$ ,  $3N\theta^2(1-\theta)$ , and  $N\theta^3$ , where  $N$  represents the total number of FH units where the base structure exists and  $\theta$  is the coverage of Kr at the center adatom site in those FH units. The calculated random distribution is shown by the black line.

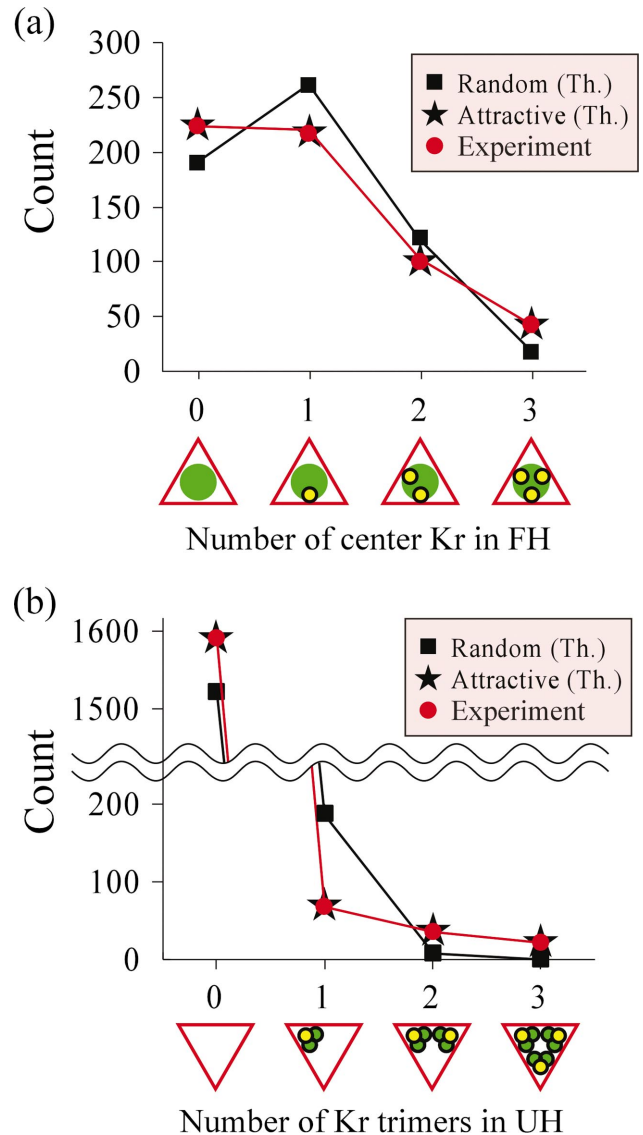


FIG. 4. (Color) (a) Number of Kr atoms at the center adatom sites in a FH unit. Theoretical results are calculations obtained for the distributions of similar types with the assumption of random-site adsorption (■) and a small attractive interaction (★), respectively. (b) similar analysis performed for the number of Kr trimers in a UH unit.

The difference between experimental and theoretical results is clear, indicating the existence of a certain attractive interaction between adsorbates, despite their separate adsorption form instead of clustering.

Next, the correlation between the rare gases in the neighboring  $7 \times 7$  half-units is discussed. We selected all UH units occupied by at least one Kr atom and classified them according to the number of neighboring FH units that contains at least one Kr atom. A UH unit cell has three neighboring FH unit cells. Thus, all UH units with Kr atoms are classified into four types (from type 0 to type 3), which are illustrated in Fig. 5 below the graph. As in the case of intra-half-unit interaction, distribution was plotted for these four types (red line) and the random distribution was calculated using measured coverage (black line). It is clear that the occurrence of

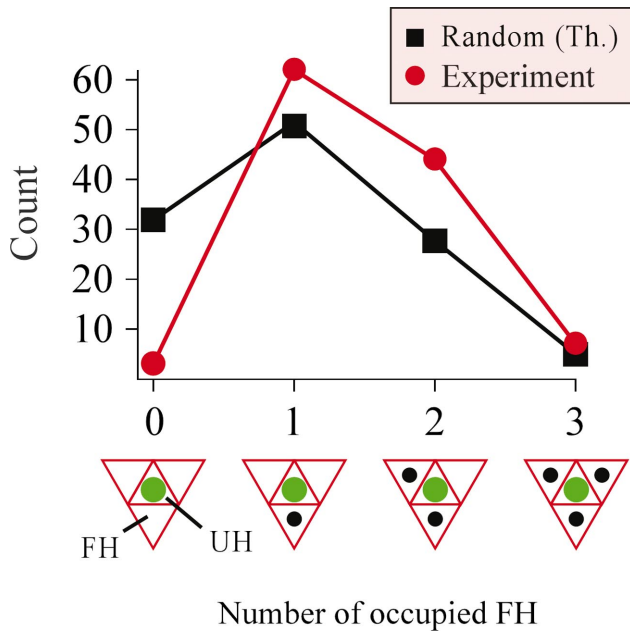


FIG. 5. (Color) Number of Kr adsorbed FH units which surround a UH unit.

type 0 is less frequent in the experiment, and vice versa for types 1, 2, and 3. This again indicates the existence of an attractive interaction between Kr atoms even across the  $7 \times 7$  units.

The complete understanding of an epitaxial system may be difficult, unless an *ab initio* calculation is done. However, it is very difficult to perform a full calculation on an adsorbate of high  $Z$  number with a large unit cell size. Therefore, we performed a simulation assuming a small attractive interaction among Kr atoms. The interaction energies for each Kr atom in a unit cell that includes one, two, and three Kr atoms are defined as  $E_1$ ,  $E_2$ , and  $E_3$ , respectively, where  $E_3 < E_2 < E_1$ . Then, the total free energies are reduced by clustering as  $dE = 2(E_1 - E_2) = -2dE_{12}$  and  $dE = 3(E_1 - E_3) = -3dE_{13}$  for a half unit cell with two and three Kr atoms, respectively. The experimental distribution was reproduced within 1% accuracy with the parameters of  $dE_{12} = -0.18$  and  $dE_{13} = -0.57$ , here thermal energy  $k_B T$  is used as the

unit. This indicates that an attractive interaction exists among Kr atoms in the adsorption process, resulting in less frequent occurrences of types 1 and 2. A similar analysis was performed for the number of Kr trimers in a UH unit [Fig. 4(b)]. For the case of trimers, the values are  $dE_{12} = -1.8$  and  $dE_{13} = -2.8$ .

The value calculated by the Lennard-Jones potential using the parameters of  $\epsilon = 160$  K and  $\sigma = 0.338$  nm and the distance 0.77 nm is  $-0.29k_B T$ , which is close to the obtained values. However, the noteworthy point is that Kr atoms do not form clusters and are adsorbed separately. That is, the interaction energy becomes larger in a cluster form at a distance of  $\sim 0.4$  nm; however, even a dimer does not exist at the center adatom sites, suggesting the existence of an interaction different from the simple van der Waals interaction. The apparent temperature may be higher than  $\sim 10$  K due to the influence of a tip sample interaction. In such a case, the energies we estimated become higher, and does the mechanism more comprehensive. Another remarkable point is that the energy is not a simple additional form.

As pointed out earlier by Lang *et al.* in the jellium model, noble gas adsorbates on metallic or semiconducting substrates can be model systems for understanding a general adsorption problem.<sup>7</sup> Kr may not be a simple atom with van der Waals interaction but an atom interacting with substrate. A similar tendency of the attractive interaction was also observed for Xe, as shown in Fig. 1 of Ref. 6. Since the energy is not a simple additional form, a many body effect may need to be taken into account even in such a case.<sup>8</sup> Further study is necessary to clarify the interaction in more detail.

The weak interaction may become an advantage for probing the subtle change in the surface electronic structure. In fact, for example, alkali metals are known to induce a strong charge transfer.<sup>9,10</sup> In such a case, although site-dependent adsorption occurs, the change in the electronic structure cannot be clearly detected by the subsequent atoms. A complete understanding of the adsorption mechanism will allow rare gases to be used as a sensitive probe on the nanoscale.

This work was supported by Grant-in-Aid for Scientific Research from the Ministry of Education, Science, Sports and Culture of Japan.

\*Present address: Tribology group, AIST, Tsukuba, 305-8564, Japan

†Corresponding author. Email address: hidemi@ims.tsukuba.ac.jp <http://dora.ims.tsukuba.ac.jp/>

<sup>1</sup>J. Park, S. Kahng, U. Ham, Y. Kuk, K. Miyake, K. Hata, and H. Shigekawa, Phys. Rev. B **60**, 16 934 (1999).

<sup>2</sup>P. Zeppenfeld, S. Horch, and G. Comsa, Phys. Rev. Lett. **73**, 1259 (1994).

<sup>3</sup>S. Horch, P. Zeppenfeld, and G. Comsa, Appl. Phys. A: Mater. Sci. Process. **60**, 147 (1995).

<sup>4</sup>Y. Li, K. Miyake, O. Takeuchi, D. Futaba, M. Matsumoto, T. Okano, and H. Shigekawa, Jpn. J. Appl. Phys. **40**, 4399 (2001).

<sup>5</sup>J. Park, U. Ham, S. Kahng, Y. Kuk, K. Miyake, K. Hata, and H.

Shigekawa, Phys. Rev. B **62**, 16 341 (2000).

<sup>6</sup>Y. Li, O. Takeuchi, D. Futaba, H. Oigawa, K. Miyake, H. Shigekawa, and Y. Kuk, Phys. Rev. B **65**, 113306 (2002).

<sup>7</sup>D. Eigler, P. Weiss, E. Schweizer, and N. Lang, Phys. Rev. Lett. **66**, 1189 (1991).

<sup>8</sup>K. Rosciszewski, B. Paulus, P. Fulde, and H. Stoll, Phys. Rev. B **62**, 5482 (2000).

<sup>9</sup>T. Hashizume, K. Motai, Y. Hasegawa, I. Sumita, H. Tanaka, S. Amano, S. Hyodo, and T. Sakurai, J. Vac. Sci. Technol. B **9**, 745 (1991).

<sup>10</sup>Y. Ma, C. Chen, G. Meigs, F. Sette, G. Illing, and H. Shigekawa, Phys. Rev. B **45**, 5961 (1992).